Competition between α, β, and γ Polymorphs in a β-Nucleated Metallocenic Isotactic Polypropylene

Rachida Krache,[†] **Rosario Benavente,**[‡] **Juan M. López-Majada,**[‡] **José M. Pereña,**[‡] **María L. Cerrada,**[‡] **and Ernesto Pérez*,**[‡]

LMPM, Département de Génie des Procédes, Faculté des Sciences de L'ingénieur, Université Ferhat Abbes, Sétif 19000, Algeria, and Instituto de Ciencia y Tecnología de Polímeros (CSIC), Juan de la Cierva 3, 28006-Madrid, Spain

ABSTRACT: The competition between α, β, and γ polymorphs has been studied in a β-nucleated metallocenic isotactic polypropylene, iPP, as a function of the cooling rate and of the isothermal crystallization temperature, by performing X-ray diffraction and DSC experiments. It was found that the addition of a 1% by weight of a typical β-nucleating agent is not enough to develop any appreciable amount of β modification, at least under the crystallization conditions used, which cover a wide range of cooling rates. In comparison, the same amount of nucleating agent added to a Ziegler−Natta iPP leads to almost 100% of β form at low cooling rates. It seems that such amount of β nucleating agent is not enough to counterbalance the well-known γ nucleation ability of the relatively high content of defects (stereo- and regioerrors) which are present in the studied metallocenic iPP, and only different proportions of γ and α modifications are obtained in this sample, the relative amount of them depending on the cooling rate. On the contrary, if a 5% nucleating agent is added, the β modification is also obtained, in addition to the γ and α polymorphs. However, now the amount of β crystals as a function of the cooling rate follows a trend opposite to that for the Ziegler−Natta iPP: the higher are the cooling rates (or the lower are the isothermal crystallization temperatures) the larger proportions of β modification are obtained. It is deduced, therefore, that the nucleation ability of the chain errors which leads to the development of the γ form predominates over that one of the β nucleating agent. The enthalpies for the 100% crystalline modifications, estimated from the enthalpies of melting and from the X-ray determined proportions of the different polymorphs, are rather similar: 162, 159, and 158 J/g for the α, β and γ phases, respectively. These values are inside the experimental error.

Introduction

Isotactic polypropylene, iPP, is one of the most important thermoplastic polymers owing to its low manufacturing cost and rather versatile properties. Moreover, iPP exhibits a very interesting polymorphic behavior, depending on the polymerization procedure, thermal history and use of different nucleants. Thus, three different polymorphic modifications, α, β, and γ, all sharing a 3-fold conformation,[1−4] have been reported. In addition, fast quenching of iPP leads to a phase of intermediate or mesomorphic order.[1,4−9]

The monoclinic α form[10] is the most common and stable modification, being found in all kinds of solution-crystallized iPP samples and also in most melt-crystallized specimens.[1,2,4,10,11] The trigonal β modification[12,13] is a metastable phase that does not appear on the phase diagram,[14,15] and it is produced only under special crystallization conditions or in the presence of selective β nucleating agents.[1−4,16−18] The orthorhombic γ form[19] has been found in the case of low-molecular weight iPP and in random copolymers of propylene and α-olefins,[1,2,4,11,20] or by the effect of pressure.[14,15,21,22] Moreover, the γ modification is especially favored in the case of iPP synthesized by metallocene catalysts, because of the presence of errors homogeneously distributed among the different polymer chains.[23−26]

Different specific nucleating agents are usually added to iPP in order to provide additional nucleation sites for the crystal-lization, resulting on increased crystallization rates and reduced spherulite sizes. Moreover, as commented above, certain nucleating agents promote the formation of the β modification, which is reported to have some interesting properties, namely a better impact strength and toughness than those for the α modification.[18] Moreover, the β modification of iPP is also specially interesting since it was the first example of a frustrated structure in polymer crystallography.[2]

Most of the studies related to the achievement of the β modification refer to traditional Ziegler−Natta iPP, where the β form is produced at the expenses of the α modification. On the contrary, to our knowledge, very few studies[27,28] are concerned with metallocenic iPP, where the γ modification is also competing with the α form. This competition may have an important influence on the ability to obtain the β polymorph, as it will be shown.

The aim of this work is to analyze the effect of crystallization conditions (cooling rate and isothermal crystallization temperature) on the relative proportions of α, β, and γ modifications obtained in a metallocenic iPP additivated with a specific β nucleating agent. For comparison, a traditional Ziegler−Natta iPP is also studied under similar conditions and with the same nucleating agent.

Experimental Part

Two commercial iPP resins have been used: a metallocenic one (m-iPP) from Basell, and a traditional Ziegler−Natta polymer (z-iPP) supplied by Repsol-YPF. The characteristics of the two polymers are shown in Table 1.

The β nucleating agent is a mixture of pimelic acid and calcium stearate (in a 1:2 proportion), supplied by Fluka. This is known to

* Corresponding author. E-mail: ernestop@ictp.csic.es.
† LMPM, Département de Génie des Procédes, Faculté des Sciences de L'ingénieur, Université Ferhat Abbes.
‡ Instituto de Ciencia y Tecnología de Polímeros (CSIC).

Table 1. Characteristics of the Two iPP Samples

sample	% [mmmm]	stereo defects (%)	regio[a] defects (%)	total defects (%)	$10^{-3}M_w$	M_w/M_n	MFI[b]
m-iPP	94.3	0.94	0.89	1.83	180	2.1	60
z-iPP	91.8				349	4.0	8.5

[a] 2,1 errors, since 1,3 regio-errors have not been detected   [b] 230 °C/2.16 kg

be a highly selective β nucleator.[29,30] The iPP resins were blended with contents in nucleating agent of 1 or 5 wt % by using a Haake Rheocord 9000 internal mixer, at 180 °C and 40 rpm for 10 min.

Films were obtained by compression molding in a Collin press between hot plates (200 °C for z-iPP and 190 °C for m-iPP) at a pressure of 10 MPa for 4 min. Two different thermal treatments were applied. The first thermal history, labeled S, consisted of a slow cooling (ca. 1.5 °C/min) from the molten state down to room temperature, at the inherent cooling rate of the press, after the power was switched off. The second one, named Q, applied a fast quench (ca. 200 °C/min) between plates refrigerated with cold water after the melting of the material in the press. The specimens for the different samples and content of nucleating agent are designated as follows: the letter *z* or *m* for the Ziegler–Natta or the metallocenic iPP, respectively, followed by the weight percentage of nucleating agent and the corresponding code for the cooling conditions. For instance, m5Q designates a metallocenic iPP specimen with a 5% of nucleating agent and quenched from the melt in the press.

Parts of those films were also used to prepare different specimens by cooling from the melt at controlled rates in a Mettler FP82HT hot stage. In these cases, the specimens designation is as before, but with the letter *c* followed by the cooling rate (in °C/min). Thus, z1c20 indicates a Ziegler–Natta iPP specimen, with a 1% nucleating agent, and cooled from the melt in the Mettler hot stage at a rate of 20 °C/min.

Finally, other specimens were prepared by cooling from the melt directly to room temperature by removing the molten sample from the hot stage. These specimens will be named as qRT, and the estimated cooling rate is around 100 °C/min.

The thermal properties of the different specimens were analyzed in a Perkin-Elmer DSC-7 calorimeter connected to a cooling system and calibrated with different standards. The sample weight ranged from 6 to 9 mg, and a heating rate of 20 °C/min was used.

Wide-angle X-ray scattering (WAXS) patterns were recorded in the reflection mode, at room temperature, by using a Philips diffractometer with a Geiger counter connected to a computer. Ni-filtered Cu Kα radiation was used. The diffraction scans were collected over a period of 20 min in the 2θ range from 3 to 43°, with a sampling rate of 1 Hz. The goniometer was calibrated with a silicon standard.

The X-ray determinations of the degree of crystallinity were performed by subtraction of the corresponding amorphous component by comparison with the totally amorphous profile of an elastomeric PP sample.[31,32]

The X-ray diffraction experiments with synchrotron radiation were carried out at the soft-condensed matter beamline A2 at Hasylab (Hamburg, Germany), with a monochromatized wavelength of 0.150 nm. A linear position-sensitive detector was used, covering the approximate 2θ range of 10–30°. The calibration of the spacings was performed by employing the diffractions of a crystalline PET specimen. Film samples of about 20 mg were covered with aluminum foil to ensure homogeneous heating or cooling and were placed in the temperature controller of the line in vacuum.

Results and Discussion

Variable Cooling Rate Experiments. An initial set of experiments was carried out in the m1 specimens, i.e., those from the metallocenic iPP with 1% of the nucleating agent. The X-ray diffractograms corresponding to the different specimens are shown in Figure 1. Surprisingly, and despite the relatively high content of nucleating agent, no sign of the β modification is observed, which is characterized by a strong reflection at 2θ = 16.1°. On the contrary, different proportions of γ and α

modification are obtained, with the γ content increasing with decreasing cooling rates, as expected.[23,24]

In order to check that there was no problem with the nucleating agent and/or the preparation conditions, a second set of specimens was prepared from the Ziegler–Natta polymer, also with 1% of a nucleating agent. The corresponding X-ray diffractograms are presented in Figure 2. It is now evident that for the non-quenched samples the majority of the crystals are of the β type, with the characteristic reflections of the trigonal β modification appearing at 16.1 and 21.2°, respectively. Moreover, the β content decreases very much as a more effective quenching is applied, as expected.[17]

Taking into account all the previous results, a third set of specimens was prepared, with the metallocenic iPP but now with 5% of a nucleating agent. The corresponding X-ray diffractograms are shown in Figure 3. The behavior is rather interesting, since different proportions of the three modifications are obtained, depending on the cooling rate. Thus, and similarly to the m1 specimens, the γ modification is predominant at low cooling rates, but the majority of the crystals are now of the β type in the quenched specimens. This behavior is opposite to that found for the z1 samples, where higher proportions of β crystals are obtained for the lower cooling rates (see Figure 2).

The explanation may be found in the specific characteristics of the metallocenic iPP chains, where a uniform concentration of defects (stereo- and regioerrors) is present throughout the different macromolecules. It has been reported[24,26,33] that the development of the γ phase is favored by interrupting isotactic segments, so that the maximum content of γ modification that can be formed is directly proportional to the concentration of those defects, i.e., inversely proportional to the average length of isotactic sequences. Moreover, the proportion of γ crystals is also dependent on the crystallization conditions, and it diminishes very much at low crystallization temperatures[24,26] or high cooling rates.[23]

The present metallocenic iPP polymer is found to have a 0.94% of stereo defects and a 0.89% of 2,1 regioerrors (see Table 1), while no 1,3 regioerrors have been detected. Therefore, the total number of defects amounts to 1.83%, and, from this value and the other data in Table 1, the average length of isotactic sequences is calculated[24] to be around 52, a relatively small value that explains the high proportions of γ modification that can be obtained in the present m-iPP sample.

Moreover, the fact that the total number of defects, 1.83%, of the m-iPP sample is relatively high, may be responsible for the impossibility of observing the β modification in those specimens (at least under the crystallization conditions employed here). It seems that we need an amount of nucleating agent high enough in order to overwhelm the strong tendency to obtain the γ form, and then considerable amounts of β modification can be observed, as it happens in the m5 specimens. Evidently, different metallocene iPP samples with varying concentration of defects and different concentrations of nucleating agent should be explored to ascertain this conclusion. We have found only two literature reports[27,28] concerning the achievement of the β modification in metallocenic iPP homopolymers. The concentration of defects is reported in one of those papers,[27] which deals with a polymer with a considerably lower concentration of
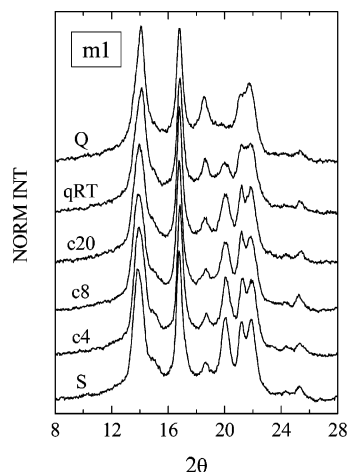
Figure 1. X-ray diffractograms, at room temperature, for the m1 specimens at the indicated crystallization conditions.
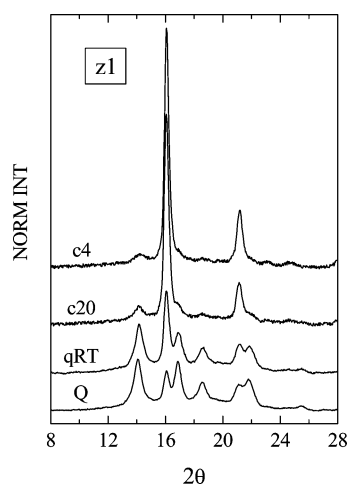

Figure 2. X-ray diffractograms, at room temperature, for the z1 specimens at the indicated crystallization conditions. For better visualization, the order of the diagrams in this figure is opposite to that in Figures 1 and 3.

Figure 3. X-ray diffractograms, at room temperature, for the m5 specimens at the indicated crystallization conditions.

Table 2. X-ray Determined Overall Degree of Crystallinity, Percentage of Each Modification, Normalized[a] Total Enthalpy of Melting and Enthalpy Corresponding to the 100 Crystal Considering the WAXS Crystallinity

specimen	f_c^{WAXS}	% of each form			ΔH (J/g)	$\Delta H^{100\% \text{ WAXS}}$ (J/g)
		β	α	γ		
m1Q	0.56	0	72	28	89	159
m1qRT	0.57	0	49	51	89.5	157
m1c20	0.59	0	31	69	92	156
m1c8	0.60	0	28	72	93.5	156
m1c4	0.61	0	24	76	95	156
m1S	0.63	0	22	78	99.5	158
m5Q	0.55	71	20	9	86	156
m5qRT	0.56	54	31	15	87	155
m5c20	0.59	19	36	45	88.5	150
m5c8	0.59	12	35	53	91.5	155
m5c4	0.61	8	34	58	91.5	150
m5S	0.62	3	26	71	98	158
z1Q	0.60	12	88	0	97	162
z1qRT	0.61	29	71	0	98.5	161
z1c20	0.65	82	18	0	104	160
z1c4	0.66	91	9	0	107.5	161

[a] Normalized to the actual iPP content in the specimen.

defects, so that lower proportions of γ form are obtained in the raw polymer, and the β modification can be observed at a much lower concentration of nucleating agent, this agent being different to the one used here.

Moreover, high proportions of β modification are also observed in metallocenic iPP by the combined effect of β nucleators and high pressures,[34] or in the case of copolymers.[35]

The proportion of the phases present in the different specimens here analyzed can be determined from the deconvolution of the diffractograms shown in Figures 1, 2, and 3. The more appropriate procedure may be the following: first, the amount of amorphous phase can be determined from the comparison with the diffraction profile corresponding to a totally amorphous, elastomeric, polypropylene sample, obtained in the same diffractometer and configuration.[31] In this way, the total X-ray crystallinity was determined, and the corresponding values are presented in Table 2. It can be observed that the degree of crystallinity is around 0.05−0.07 units lower for the metallocenic iPP specimens. The more random distribution of defects in metallocenic iPP is responsible for those lower values, as well as for the lower melting temperatures (see below).

Moreover, the diffractograms representing the pure crystalline components of each specimen have been obtained from the subtraction of the scaled amorphous profile. These pure crystal profiles can be used for the subsequent deconvolution of the
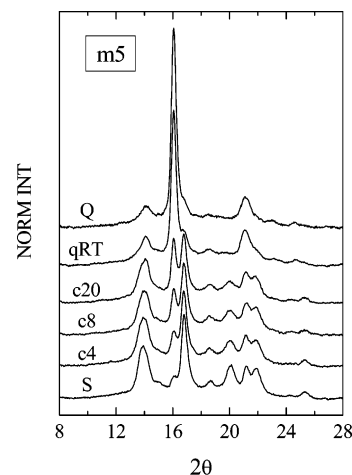
diffraction peaks corresponding to each modification, so that the proportion of the different forms can be determined. The present diffraction peaks are fitted to Voigt profiles as one of the best options.

With this procedure, the proportions of the various modifications for the different specimens are those presented in Table 2. It is important to subtract first the amorphous component, since it shows a clearly asymmetric profile,[31] with a maximum at 2θ around 15.5° and a shoulder centered at around 20°.

On the other hand, those pure crystal profiles, with varying amounts of α, β, and γ modifications, can be used for obtaining the diffraction profiles corresponding to each modification exclusively, by appropriate linear combination of the different profiles. In principle, this seems to be a straightforward procedure. However, a certain degree of uncertainty arises from the fact that those profiles correspond to samples crystallized under varying conditions, so that the diffraction peaks display slightly different widths, the width being smaller for the lower crystallization rates, as corresponds to more perfect, thicker crystals.

Anyway, the appropriate linear combinations lead to the pure profiles shown in Figure 4 for the three pure modifications, where the corresponding Miller indices are also presented. The pure profiles allow checking the validity of the expression
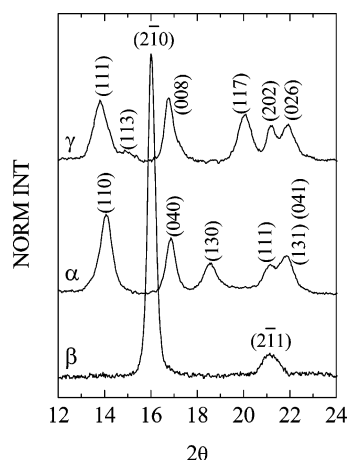
Figure 4. X-ray diffractograms corresponding to the three pure crystal modifications. The Miller indices are indicated.

commonly used for the determination of the β fraction, which reads:[11]

$$K_\beta = \frac{H_{\beta 1}}{H_{\beta 1} + (H_{\alpha 1} + H_{\alpha 2} + H_{\alpha 3})}$$

where $H_{\beta 1}$ is the height of the strongest β diffraction at around 16.1°, the $(2\bar{1}0)$ diffraction, and $H_{\alpha 1}$, $H_{\alpha 2}$, and $H_{\alpha 3}$ are the heights of the three first α peaks, appearing at around 14.1, 16.9, and 18.6°, respectively, corresponding to the (110), (040), and (130) diffractions, respectively, of the α modification. The K_β value, obtained either from the heights or from the integrated intensity of the corresponding diffraction peaks,[11,17,36] has to be recognized as a relative measure of the proportion of β modification, since it includes in the calculation only selected peaks instead of the entire collection of diffractions. A similar argument applies to other proposed methods.[34]

The validity of that equation can be readily checked by determining the ratio between the intensity of the selected diffractions over the total diffractogram intensity. The values deduced from Figure 4 (considering also the small diffractions appearing at higher angles, not shown in Figure 4) are the following: 0.80 ± 0.03 for the ratio of the $\beta 1$ peak over the entire diffractogram, and 0.65 ± 0.03 for the one corresponding to the first three α peaks over the total.

It follows, therefore, that the K_β values are not representing the actual proportion of β crystals, and now that computer facilities are readily available, the consideration of all the diffraction peaks is more appropriate for determining the proportion of the different polymorphs, as it has been made for calculating the values presented in Table 2.

The relative proportions of each modification, at room temperature, for the different polymers and specimens are plotted in Figure 5 as a function of decreasing cooling rates. The upper frame corresponds to the z1 specimens. A clear increase of the β component is observed as the cooling rate decreases (as the crystallization range takes place at higher temperatures), reaching a value of more than 90% for the lowest cooling rate. Evidently, the increase of the β proportion in this case is at the expenses of the α modification.

Regarding the m1 specimens (middle frame in Figure 5), no identifiable β crystals were observed for any of the tested cooling rates, as commented above. Now, the competition is between the γ and α modifications, and at the lower cooling rates the majority of the crystals are of the γ type, although it seems that an asymptotic value of around 80% will be reached.
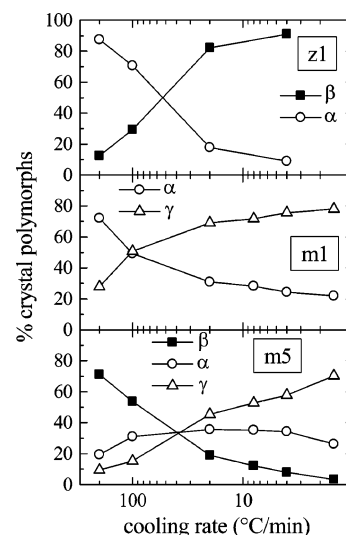

Figure 5. Relative proportions of the different polymorphs as a function of the cooling rate, for the z1 (upper frame), m1 (middle frame), and m5 (lower frame) specimens.

It has been reported[24,26] that there is a relation between the maximum amount of γ form that can be obtained and the average length of isotactic sequences. The maximum value reported here, 78%, is slightly higher than those reported before[24,26] for the actual average length of isotactic sequences. The reason may be the somewhat more refined method used here for determining the proportions of the different polymorphs.

Much more interesting is the behavior of the m5 specimens, as observed in the lower frame of Figure 5. The three polymorphs have been obtained in all the conditions analyzed. Thus, at low cooling rates the proportion of β crystals is rather small, but appreciable, while that for the α modification is nearly the same as the one obtained in the m1 specimens. It seems, therefore, that at those low cooling rates the formation of the β crystals is at the expenses of the γ modification. However, at high cooling rates the majority of the crystals are those of β type, and, evidently, they have been formed at the expenses of both the γ and α modifications.

The conclusion from this study, limited to only one type of metallocenic iPP and to only two concentrations of a particular nucleating agent, is the following: the nucleation ability of the chain errors that leads to the development of the γ form predominates over that one of the β nucleating agent. Accordingly, the β modification is only obtained in high proportions when this agent is in contents high enough and when the γ nucleation ability of the errors diminishes, i.e., at high cooling rates.

Anyway, it is interesting to note that opposite trends are obtained for Ziegler–Natta and metallocenic iPPs: the proportion of β crystals increases as the cooling rate decreases in z-iPP, but it does so when the cooling rate increases in m-iPP.

Isothermal Experiments. In order to have a better understanding on the effect of crystallization conditions, an additional analysis has been carried out by performing isothermal experiments in a synchrotron source. The corresponding results are shown in Figure 6. It has to be considered that these values correspond to the ones deduced from the last diffractogram of each experiment, i.e., they represent the actual proportions of each phase at the end of the crystallization experiment at the corresponding isothermal temperature. For practical reasons, these experiments are limited by two facts: the lowest crystallization temperature is restricted by the time required for temperature equilibration in the sample, so that the total
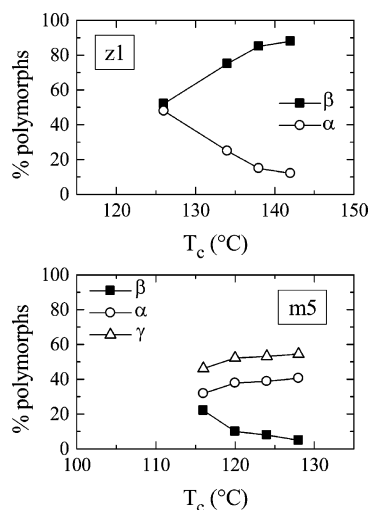
Figure 6. Relative proportions of the different polymorphs as a function of the isothermal crystallization temperature, for the z1 (upper frame) and m5 (lower frame) specimens.
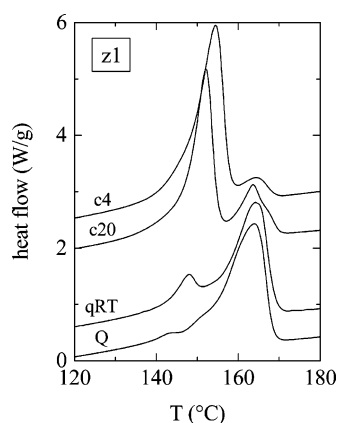

Figure 7. DSC melting curves for the z1 specimens at the indicated crystallization conditions. For better visualization, the order of the diagrams in this figure is opposite to that in Figures 8 and 9.

crystallization time shall not be smaller than around $1-2$ min. On the other hand, the crystallization times have been fixed to a maximum of around 60 min. From previous results obtained in the calorimeter, the useful range of isothermal crystallization temperatures is confined within the interval from around 126 to 142 °C for z1, and from 116 to 128 °C for m5.

It is evident from the results in Figure 6 that the conclusions from the isothermal experiments are practically the same than those extracted from the measurements after variable cooling rates. Thus, in the case of the z1 sample, higher proportions of β modification are obtained at the higher crystallization temperatures, i.e., at the lower crystallization rates, and the opposite is found for the m5 sample.

Moreover, a close inspection of Figure 6 and its comparison with Figure 5 reinforces the above-mentioned similarity, since the results deduced in the isothermal experiments match almost perfectly to those obtained at variable cooling rates in the interval from around 30 to 3 °C/min.

Thermal Behavior. The thermal behavior of the different samples has been also analyzed. Thus, Figure 7 shows the DSC melting curves corresponding to the z1 specimens. Focusing the attention on the sample crystallized at 4 °C/min, it presents a main melting endotherm at 154 °C, and a smaller one at 164 °C, assigned to the melting of the β and α crystals, respectively. The Q specimen, however, shows almost practi-

cally the high-temperature endotherm, as corresponds to a sample of around 90% α crystals. The low-temperature region presents a barely seen peak at around 143 °C, which may correspond to the melting of a small fraction of thin β crystallites, presumably formed at high undercoolings when quenching.

Although the relative intensities of the two endotherms reflect somehow the ratio of β and α crystals initially present in the sample (deduced from Figure 2), it is well-known that the β modification undergoes an important recrystallization into the α form,[17] specially when the samples, as it happens here, have been cooled down below the so-called critical temperature[17] (105 °C). The implication is that the determination from the melting endotherms of the relative proportion of each modification in the initial sample is not straightforward, although the recrystallization may be not very significant in the present case, since the melting curves have been recorded at 20 °C/min.

A certain idea of the recrystallization may be extracted, for instance, from the comparison of the melting curves for specimens z1c4 and z1c20 in Figure 7. Since the recrystallization ability of the β form is expected to be enhanced in the more imperfect crystals, that recrystallization will be, in principle, more important in specimen z1c20. In fact, the double melting peak of the α endotherm may be due to the melting of the initial α crystals and those recrystallized from the β phase. The whole α endotherm comprises around 23% of the total enthalpy, while its high-temperature component involves around 5%. Considering that the percentage of α phase deduced from the X-ray diffractogram is 18% (see Table 2), one may conclude that the high-temperature component of the α endotherm arises from recrystallization of β crystals. However, we cannot disregard the possibility of that high-temperature component arising from the recrystallization of the own α crystals. Real-time variable-temperature diffraction experiments employing synchrotron radiation are envisaged in order to solve this question.

On the other hand, the α endotherm for specimen z1c4 comprises around 9% of the total enthalpy, i.e., exactly the same percentage than the one deduced from the X-ray diffractogram. And now it seems that the α endotherm is not split, indicating that the recrystallization is not so evident, as it may be expected considering that more perfect crystals (α and β) are formed at this slow cooling rate.

Anyway, the DSC results are in agreement with the previously commented X-ray diffraction findings: the majority of the crystals are α-type in the quenched specimens, while they are β-type in those samples crystallized at low cooling rates.

Figure 8 shows the melting curves for the m1 specimens. These results also agree with the X-ray findings, since the curves show now the two endotherms typical of the melting of varying proportions of γ and α crystals, the α melting endotherm appearing at a higher temperature and with a decreasing intensity as the cooling rate decreases.

The melting curves for the m5 specimens are shown in Figure 9. The melting patterns are, evidently, rather complicated, because of the presence of the three modifications. Moreover, significant recrystallizations are evident in the quenched specimens, since four peaks or shoulders are observed, and none of them seems to correspond to the melting of the very small amount of γ-type crystals present in those specimens.

Considering the difficulty for the deconvolution of the melting curves into the different components, only the total enthalpy of melting has been determined for each specimen. The corre-
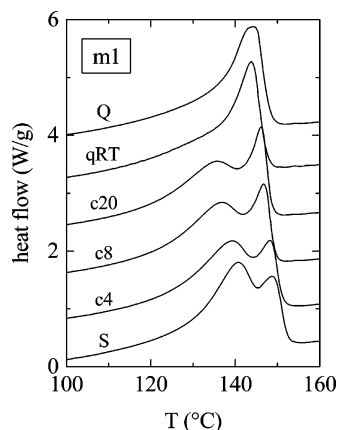
Figure 8. DSC melting curves for the m1 specimens at the indicated crystallization conditions.
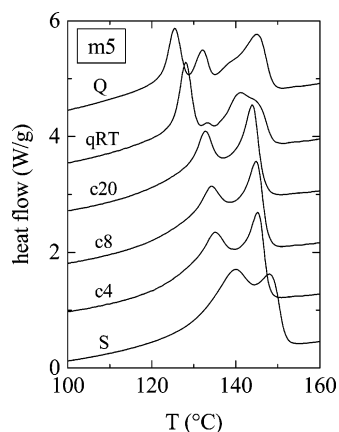

Figure 9. DSC melting curves for the m5 specimens at the indicated crystallization conditions.

sponding results, after normalization to the actual iPP content in the samples, are presented in Table 2.

At this point, it is possible to estimate the overall enthalpy of the 100% crystalline samples by considering the total enthalpy of melting and the corresponding WAXS-determined crystallinity. The values for this overall enthalpy, designated as $\Delta H^{100\% \text{ WAXS}}$, are shown in the last column of Table 2. All the values lie in the interval from 150 to 162 J/g, which is practically inside the experimental error when considering that the estimated uncertainties on the WAXS crystallinity and on the total enthalpy of melting are around ±0.02 units and ±1 J/g, respectively.

Since our specimens display very different contents on the three polymorphs, a preliminary conclusion from all these results is that the enthalpies of melting of the three modifications cannot be very different.

The values reported in the literature for $\Delta H^{100\% \text{ WAXS}}$ are the following: 167 J/g for the α modification[14,37] (although a scattering from 138 to 221 J/g can be found[17]) and 150 J/g for the γ phase.[14] Our previous results[38,39] indicate also a value around 164 J/g for the α polymorph. Regarding the β form, an enthalpy of 113 J/g is generally quoted,[17,28] although some experimental results seem to indicate that the real value should be higher.[28]

In the present case, and considering the overall enthalpies and the corresponding percentages of each modification, a set of equations can be postulated, with the three unknowns of the enthalpies for each polymorph. By appropriate linear combinations, the solution of that system leads to the following values: 162 ± 10, 159 ± 10, and 158 ± 10 J/g for $\Delta H^{100\% \text{ WAXS}}$ of the α, β and γ phases, respectively. As anticipated before, these
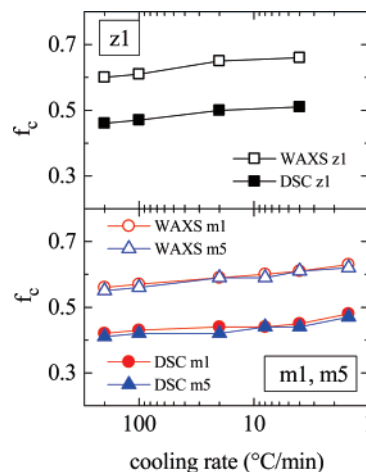

Figure 10. WAXS-determined and DSC-determined degrees of crystallinity as a function of the cooling rate for the different samples.

enthalpies are not very different, even the one for the β modification.

However, there is an important drawback for the previous calculations: they rely on the premise that what is determined as crystal from the WAXS measurements will contribute in a directly proportional way to the enthalpy. Evidently, this premise may be wrong if it is considered that there is an intermediate region, the interphase, where the physical properties of the crystal are smoothly transformed into those ones of the disordered amorphous regions. This interphase may contribute differently to the WAXS crystallinity or to the enthalpy, thus leading to different values of the crystallinity by the two techniques: X-rays and DSC.

These concepts have been invoked[40] to explain the crystallinity differences between those two techniques in iPP, since the DSC results were determined to be considerably smaller when the enthalpy of the 100% crystalline polymer (in the α modification) is taken as 209 J/g, obtained from data in polymer−diluent systems[41,42] This is the most cited value for the enthalpy of melting of a perfect iPP crystal, but, evidently, has been determined with a third, different, technique, so that it may imply new disadvantages. Anyway, if the true value of the 100% α crystals is 209 J/g instead of the 162 J/g obtained here by using the WAXS crystallinity, the enthalpies of the other two polymorphs may be scaled, most probably, in a rather similar proportion, so that the enthalpies for the β and γ modifications will be 205 and 203 J/g, respectively. With these values, the DSC crystallinities can be estimated. The corresponding values are plotted in Figure 10, compared with the WAXS crystallinities. It can be observed that in all the cases the DSC values are around 0.16 units lower than the WAXS crystallinities, in good agreement with the previous results.[40]

A final issue is the effect of the nucleant on the crystallization rate, which can be estimated just from the DSC crystallization exotherm on cooling from the isotropic melt. The corresponding DSC curves, at a cooling rate of 20 °C/min, are shown in Figure 11. The upper part represents the curves for z-iPP, and it can be observed that there is a rather important nucleating effect, since the crystallization exotherm appears at 121 °C for the specimen with 1% of a nucleating agent, a value 13 °C higher than the one exhibited by the raw z-iPP sample.

The behavior is just opposite in the case of the m-iPP specimens, as observed in the lower part of Figure 11. Thus, the raw polymer presents the crystallization exotherm at
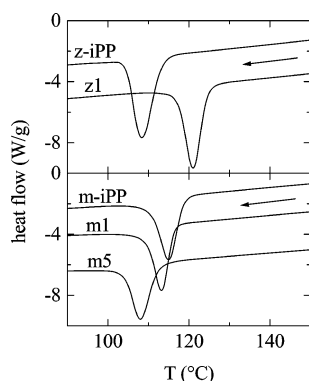
Figure 11. DSC curves on cooling from the melt at 20 °C/min for the indicated samples.

115 °C, while it appears at 113 °C for the m1 specimen, and at 108 °C for the m5 sample. Therefore, in the case of the metallocenic iPP, the β nucleating agent actually delays the crystallization (as it has been also observed when analyzing the isothermal crystallization rate for these specimens).

It is interesting to note that these crystallization exotherms show only a single peak, in spite of the formation of the different modifications. It follows, therefore, that the formation of the various polymorphs occurs rather simultaneously.

Conclusions

The addition to a metallocenic iPP of a 1% by weight of a typical β-nucleating agent is not enough to develop any appreciable amount of β modification, at least under the crystallization conditions used, which cover a wide range of cooling rates. By comparison, the same amount of nucleating agent added to a Ziegler–Natta iPP leads to almost 100% of β form at low cooling rates. It seems, therefore, that such amount of β nucleating agent is not enough to counterbalance the well-known γ nucleation ability of the 1.83% of defects (stereo- and regioerrors) which are present in the studied metallocenic iPP, and only different proportions of γ and α modifications are obtained in this sample, the relative amount depending on the cooling rate.

On the contrary, if a 5% nucleating agent is added, the β modification is also obtained, in addition to the γ and α polymorphs. However, now the amount of β-type crystals as a function of the cooling rate follows a trend opposite to that found for the Ziegler–Natta iPP: higher proportions of β modification are obtained at the higher cooling rates (or at the lower isothermal crystallization temperatures).

Moreover, the analysis of the crystallization exotherms on cooling from the melt indicates a real nucleating effect, as expected, by incorporation of the agent in the Ziegler–Natta iPP. Consequently, the exotherm appears in the specimen with 1% of β nucleator at a temperature 13 °C above that presented for the raw iPP sample. On the contrary, the opposite effect is found in the metallocenic iPP. Thus, the exotherms for the specimens with β nucleator appear at temperatures lower than that for the raw polymer. Therefore, the β nucleating agent leads in this case to a retardation of the crystallization.

The enthalpies corresponding to the 100% crystalline modifications, estimated from the total enthalpy of melting and from the X-ray determined proportions of the different polymorphs, are rather similar: 162, 159, and 158 J/g for the α, β, and γ phases, respectively, values inside the experimental error, estimated to be around 10 J/g.

References and Notes

(1) Brückner, S.; Meille, S. V.; Petraccone, V.; Pirozzi, B. *Prog. Polym. Sci.* **1991**, *16*, 361.
(2) Lotz, B.; Wittmann, J. C.; Lovinger, A. J. *Polymer* **1996**, *37*, 4979.
(3) Varga, J. *J. Mater. Sci.* **1992**, *27*, 2557.
(4) Phillips, P. J.; Mezghani, K. In *The Polymeric Materials Encyclopedia*, Salamone. J. C., Ed.; CRC Press: Boca Raton, FL, 1996; Vol. 9, p 6637.
(5) Slichter, W. P.; Mandell, E. R. *J. Appl. Phys.* **1958**, *29*, 1438.
(6) Hosemann, R.; Wilke, W. *Makromol. Chem.* **1968**, *118*, 230.
(7) Grebowicz, J.; Lau, J. F.; Wunderlich, B. *J. Polym. Sci., Polym. Symp.* **1984**, *71*, 19.
(8) Corradini, P.; de Rosa, C.; Guerra, G.; Petraccone, V. *Polym. Commun.* **1989**, *30*, 281.
(9) Arranz-Andrés, J.; Benavente, R.; Pérez, E.; Cerrada, M. L. *Polym. J.* **2003**, *35*, 766.
(10) Natta, G.; Corradini, P. *Nuovo Cimento Suppl.* **1960**, *15*, 40.
(11) Turner-Jones, A.; Aizlewood, J. M.; Beckett, D. R. *Makromol. Chem.* **1964**, *75*, 134.
(12) Meille, S. V.; Ferro, D.; Brückner, S.; Lovinger, A. J.; Padden, F. J. *Macromolecules* **1994**, *27*, 2615.
(13) Lotz, B.; Kopp, S.; Dorset, D. *C. R. Acad. Sci. Paris, Ser. IIb* **1994**, *319*, 187.
(14) Mezghani, K.; Phillips, P. J. *Polymer* **1998**, *39*, 3735.
(15) Dimeska, A.; Phillips, P. J. *Polymer* **2006**, *47*, 5445.
(16) Keith, H. D.; Padden, F. J.; Walter, N. M.; Wyckoff, H. W. *J. Appl. Phys.* **1959**, *30*, 1485.
(17) Varga, J. In *Polypropylene: Structure, blends and composites*; Karger-Kocsis, J., Ed.; Chapman and Hall: London, 1995; Vol. 1, p 56.
(18) (a) Varga, J. *J. Macromol. Sci., Phys. B* **2002**, *41*, 1121. (b) Varga, J.; Ehrenstein, W. In *Polypropylene: An A-Z Reference*; Karger-Kocsis, J., Ed.; Kluwer: London, 1999; p 51.
(19) Brückner, S.; Meille, S. V. *Nature (London)* **1989**, *340*, 455.
(20) Addink, E. J.; Beintema, J. *Polymer* **1961**, *2*, 185.
(21) Bruckner, S.; Phillips, P. J.; Mezghani, K.; Meille, S. V. *Macromol. Rapid Commun.* **1997**, *18*, 1.
(22) Mezghani, K.; Phillips, P. J. *Polymer* **1997**, *38*, 5725.
(23) Pérez, E.; Zucchi, D.; Sacchi, M. C.; Forlini, F.; Bello, A. *Polymer* **1999**, *40*, 675.
(24) Alamo, R. G.; Kim, M.-H.; Galante, M. J.; Isasi, J. R.; Mandelkern, L. *Macromolecules* **1999**, *32*, 4050.
(25) Hosier, I. L.; Alamo, R. G.; Esteso, P.; Isasi, J. R.; Mandelkern, L. *Macromolecules* **2003**, *36*, 5623.
(26) De Rosa, C.; Aurienma, F.; Paolillo, M.; Resconi, L.; Camurati, I. *Macromolecules* **2005**, *38*, 9143.
(27) Busse, K.; Kressler, J.; Maier, R.-D.; Scherble, J. *Macromolecules* **2000**, *33*, 8775.
(28) Varma-Nair, M.; Agarwal, P. K. *J. Therm. Anal. Calorim.* **2000**, *59*, 483.
(29) Shi, G.; Zhang, X.; Qiu, Z. *Makromol. Chem.* **1992**, *193*, 583.
(30) Varga, J.; Mudra, I.; Ehrenstein, G. W. *J. Appl. Polym. Sci.* **1999**, *74*, 2357.
(31) Mansel, S.; Pérez, E.; Benavente, R.; Pereña, J. M.; Bello, A.; Roll, W.; Kirsten, R.; Beck, S.; Brintzinger, H.-H. *Macromol. Chem. Phys.* **1999**, *200*, 1292.
(32) Prieto, O.; Pereña, J. M.; Benavente, R.; Cerrada, M. L.; Pérez, E. *Macromol. Chem. Phys.* **2002**, *203*, 1844.
(33) Fischer, D.; Mülhaupt, R. *Macromol. Chem. Phys.* **1994**, *195*, 1433.
(34) Obadal, M.; Cermak, R.; Stoklasa, K. *Macromol. Rapid Commun.* **2005**, *26*, 1253.
(35) Juhász, P.; Varga, J.; Belina, K. *J. Macromol. Sci., Phys. B* **2002**, *41*, 1173.
(36) Davies, R. J.; Zafeiropoulos, N. E.; Schneider, K.; Roth, S. V.; Burghammer, M.; Riekel, C.; Kotek, J. C.; Stamm, M. *Colloid Polym. Sci.* **2004**, *282*, 854.

(37) Bond, E. B.; Spruiell, J. E.; Lin, J. S. *J. Polym. Sci., Part B: Polym. Phys.* **1999**, *37*, 3050.

(38) Prieto, O.; Pereña, J. M.; Benavente, R.; Pérez, E.; Cerrada, M. L. *J. Polym. Sci.: Polym. Phys.* **2003**, *41*, 1878.

(39) López-Majada, J. M.; Palza, H.; Guevara, J. L.; Quijada, R.; Martínez, M. C.; Benavente, R.; Pereña, J. M.; Pérez, E.; Cerrada, M. L. *J. Polym. Sci., Part B: Polym. Phys.* **2006**, *44*, 1253.

(40) Isasi, J. R.; Mandelkern, L.; Galante, M. J.; Alamo, R. G. *J. Polym. Sci., Part B: Polym. Phys.* **1999**, *37*, 323.

(41) Krigbaum, W. R.; Uematsu, I. *J. Polym. Sci., Part A: Polym. Chem.* **1965**, *3*, 767.

(42) Wunderlich, B. *Macromolecular Physics*; Academic Press: New York, 1980; Vol. 3.